


Original Research

GD2-Specific CAR T Cells Demonstrate Potent and Targeted Anti-Tumor Efficacy Against Melanoma *In Vitro* and *In Vivo*

Julia Philippova¹, Julia Shevchenko¹, Alaa Alsalloum¹, Marina Fisher¹, Saleh Alrhoun¹, Roman Perik-Zavodskii¹, Olga Perik-Zavodskaia¹, Julia Lopatnikova¹, Vasily Kurilin¹, Marina Volynets¹, Evgenii Zavjalov^{1,2}, Olga Solovieva^{1,2}, Hiroshi Shiku^{3,‡}, Sergey Sennikov^{1,*} 

¹Laboratory of Molecular Immunology, Federal State Budgetary Scientific Institution Research Institute of Fundamental and Clinical Immunology, 630099 Novosibirsk, Russia

²Center for Collective Usage SPF-vivarium, Institute of Cytology and Genetics, Siberian Branch of the Russian Academy of Sciences, 630090 Novosibirsk, Russia

³Department of Personalized Cancer Immunotherapy, Mie University Graduate School of Medicine, 514-8507 Tsu, Mie, Japan

*Correspondence: sennikov@niikim.ru (Sergey Sennikov)

‡Deceased.

Academic Editors: Natascia Tiso and Roberto Bei

Submitted: 14 May 2025 Revised: 14 July 2025 Accepted: 25 July 2025 Published: 25 August 2025

Abstract

Background: Disialoganglioside (GD2) is a tumor-associated antigen that is highly expressed in various neuroectodermal cancers, including melanoma. While chimeric antigen receptor (CAR) T-cell immunotherapy has demonstrated remarkable success in treating hematologic neoplasms, the identification of suitable targets remains a major obstacle in translating this approach to solid tumors. **Methods:** Peripheral blood T lymphocytes from six healthy donors were used to generate GD2-specific CAR T cells via retroviral transduction. The resulting GD2.CAR T cells were characterized by NanoString transcriptome profiling, flow cytometry with hierarchical stochastic neighbor embedding (HSNE) dimensionality reduction, and *in vitro* cytotoxicity assays against GD2⁺ and GD2[−] melanoma cell lines. *In vivo* experiments were also performed using GD2⁺ xenograft models and a single intratumoral dose of 8×10^6 GD2.CAR T cells. **Result:** The GD2.CAR T cell population exhibited a predominantly naive phenotype (CD8⁺CD40L⁺CD69[−]CD107a⁺4-1BB⁺FasL⁺) and effective anti-tumor mechanisms involving the granzyme A/B axis, the Fas/FasL axis, and cytokine release. Transcriptome analysis revealed transduction-related effects on proliferation and a shift towards an effector phenotype during early co-culture with tumor cells, accompanied by upregulation of interferon-gamma (IFN- γ) and cytokine signaling genes. GD2.CAR T cells demonstrated robust cytotoxicity against GD2⁺ melanoma cells *in vitro*, while significant *in vivo* tumor control was observed in xenograft models. **Conclusion:** GD2.CAR T cells demonstrate potent anti-tumor activity against melanoma *in vitro* and *in vivo*, highlighting their therapeutic potential and warranting further clinical investigation.

Keywords: CAR T cells; disialoganglioside; xenograft model; cytotoxicity; transcriptome profiling

1. Introduction

Melanoma is a common and aggressive cancer type originating from melanocytes and notorious for its rapid metastasis [1,2]. Although surgery, chemotherapy, and radiation remain first-line therapies, melanoma often develops resistance, and prognosis worsens at later stages [3]. Immunotherapy is a promising method that employs natural defense mechanisms to treat tumors. Adoptive cell therapy is effective in the treatment of metastatic melanoma [4], but lacks specificity in targeting tumor cells. To address this limitation, chimeric antigen receptor (CAR) T-cell therapy has been developed. Genetically engineered CAR T cells can recognize tumors in a non-major histocompatibility complex (MHC)-restricted manner without co-stimulation [5]. As a result, CAR T cells are an off-the-shelf T cell product capable of targeting specific antigens for tumor elimination. Nonetheless, the application of CAR

T-cell therapy has significant challenges in an immunosuppressive tumor microenvironment (TME) characterized by molecular, cellular, and metabolic profiles that could lead to T cell exhaustion and dysfunction [6].

The selection of a tumor-specific surface antigen that is highly expressed on tumor cells but minimally expressed on normal cells is critical for effective CAR T-cell therapy. This is essential for achieving optimal treatment outcomes and minimizing negative side effects. Disialoganglioside (GD2) is overexpressed in melanoma but shows limited expression in normal tissues [7,8]. Increased GD2 expression on melanoma cells may be associated with metastasis [9] and the malignant phenotype of melanoma [10]. Structurally, GD2 is a glycolipid expressed on the cell surface, making it a suitable target for recognition by antibodies or chimeric antigen receptors. In addition, GD2 has shown potential as a target for the development of CAR T-cell therapies against melanoma [11].



Preclinical studies have shown that GD2.CAR T cells, either alone or in combination with other therapeutic agents, can efficiently eliminate melanoma cells *in vitro* and suppress tumor growth *in vivo* [12–15]. However, a phase I clinical trial of GD2.CAR T cells demonstrated limited expansion and persistence, with T cells exhibiting an exhausted phenotype in metastatic melanoma patients, as evidenced by *ex vivo* analysis of peripheral blood samples after infusion [16]. This approach requires the development of novel methods to enhance the design of the CAR construct. Moreover, further investigations are required into the impact of the TME on CAR T cells.

In the present study, we have built upon our previous observation of antitumor activity with melanoma-associated antigen family A4 (MAGE-A4)-specific T-cell receptor (TCR)-like CAR T cells and New York esophageal squamous cell carcinoma 1 (NY-ESO-1)-specific TCR-engineered T cells [17,18] to evaluate the therapeutic potential of GD2-specific CAR T cell therapy. We utilized a previously optimized retroviral construct encoding a GD2-specific single-chain variable fragment (scFv) derived from a modified mAb 220-51, fused to human CD28 and CD3 ζ intracellular signaling domains, and incorporating a sequence encoding the glucocorticoid-induced tumor necrosis factor receptor (TNFR) family-related protein ligand (GITRL) [19]. This construct was designed to enhance antitumor activity, based on accumulating evidence that stimulation of GITR with GITRL increases TCR-induced T cell proliferation and cytokine production, reduces the threshold for CD28 co-stimulation in effector CD8⁺ T cells, and preserves T cells from anti-CD3-induced apoptosis [19,20]. Accordingly, we generated GD2-specific CAR T cells via retroviral transduction in order to further characterize their phenotype, *in vitro* function, and *in vivo* inhibition of tumor growth. The resulting GD2.CAR T cell phenotype was assessed using hierarchical stochastic neighbor embedding (HSNE) analysis. We also assessed the functional properties of these cells, including cytokine production and cytotoxic activity against melanoma cell lines *in vitro* and in a xenograft model. Furthermore, we investigated the early-stage transcriptomic changes that occur in GD2.CAR T cells upon interaction with tumor cell lines, paying particular attention to alterations in T cell memory differentiation.

2. Material and Methods

2.1 Donors

The study was carried out in accordance with the guidelines of the Declaration of Helsinki and was approved by the local ethics committee of the Research Institute of Fundamental and Clinical Immunology (protocol #139 on May 30, 2022). Healthy blood donors ($n = 6$ males, age 27.33 ± 1.63 years [mean \pm standard error of the mean (SEM)]) were recruited between June and December 2022. All donors met standard requirements for blood donation, showed no evidence of acute infection or prior blood transfusion, and provided written informed consent.

2.2 Cell Lines

The human melanoma cell line SK-MEL-37 (RRID: CVCL_3878) and patient-derived cell lines S6 and V9 were provided by Professor H. Shiku (Mie University Graduate School of Medicine, Japan). The local ethics committee of the Research Institute of Fundamental and Clinical Immunology approved the use of patient-derived cell lines S6 and V9 in this study (protocol #139 on May 30, 2022). All cell lines (SK-MEL-37, S6, and V9) tested negative for Mycoplasma (Cat. #MR004, Evrogen, Moscow, Russia), and the SK-MEL-37 cell line was validated by short tandem repeat (STR) profiling. To ensure the identity of the cell lines used, the S6 and V9 patient-derived cell lines were validated using light microscopy to confirm characteristic melanoma morphology (pleomorphism, large nuclei, variable cytoplasm, and the presence/absence of melanin pigment). Cells were cultured in RPMI-1640 medium supplemented with 10% fetal bovine serum (Cat. #RM10832-500ML, HiMedia, Maharashtra, India), 2 mM L-glutamine (Cat. #1383, Biolog, Saint Petersburg, Russia), 5×10^{-5} mM β -mercaptoethanol (Cat. #M3148, Sigma-Aldrich, Saint-Louis, MO, USA), 25 mM HEPES (Cat. #1261, Biolog, Saint Petersburg, Russia), 80 μ g/mL gentamicin (Cat. #A011p, PanEco, Moscow, Russia), and 100 μ g/mL ampicillin (Cat. #260317, Sintez, Kurgan, Russia). Cells were seeded into flasks at a concentration of $50\text{--}75 \times 10^3$ cells/mL until they reached the log phase of growth. They were then detached using trypsin-versene solution (Trypsin: Cat. #1225, Biolog, Saint Petersburg, Russia; Versene: Cat. #1232, Biolog, Saint Petersburg, Russia) for experimental use. GD2 expression on SK-MEL-37, S6, and V9 was assessed using flow cytometry with mAb 14.G2a (Cat. #357304, BioLegend, San Diego, CA, USA) according to the manufacturer's recommendations and analyzed on an Attune NxT flow cytometer (Thermo Fisher Scientific, Waltham, MA, USA) (SK-MEL-37 and S6: GD2-positive; V9: GD2-negative).

2.3 Retroviral Particles

A gamma-retroviral vector encoding a GD2-specific CAR was provided by Professor H. Shiku. The structure of the pGD2 transfer Moloney murine leukemia virus (MMLV) plasmid is shown in Fig. 1.

2.4 Generation of CAR T Cells and Retroviral Transduction

CAR T cells were generated by isolating PBMCs from healthy adult donors using Ficoll-Urografin (Cat. #17-1440-03, PanEco, Moscow, Russia) density gradient centrifugation and washed twice with PBS (Cat. #1247, Biolog, Saint Petersburg, Russia). Proliferation was stimulated by coating 12-well plates (TPP, Trasadingen, Schaffhausen, Switzerland) with 25 μ g/mL RetroNectin (Cat. #T100B, Takara Bio, Kyoto, Japan) and 5 μ g/mL anti-CD3 antibodies (Cat. #300465, Biolegend, San Diego, CA, USA). PBMCs were then plated at 0.5×10^6 cells/mL in 2 mL GT-

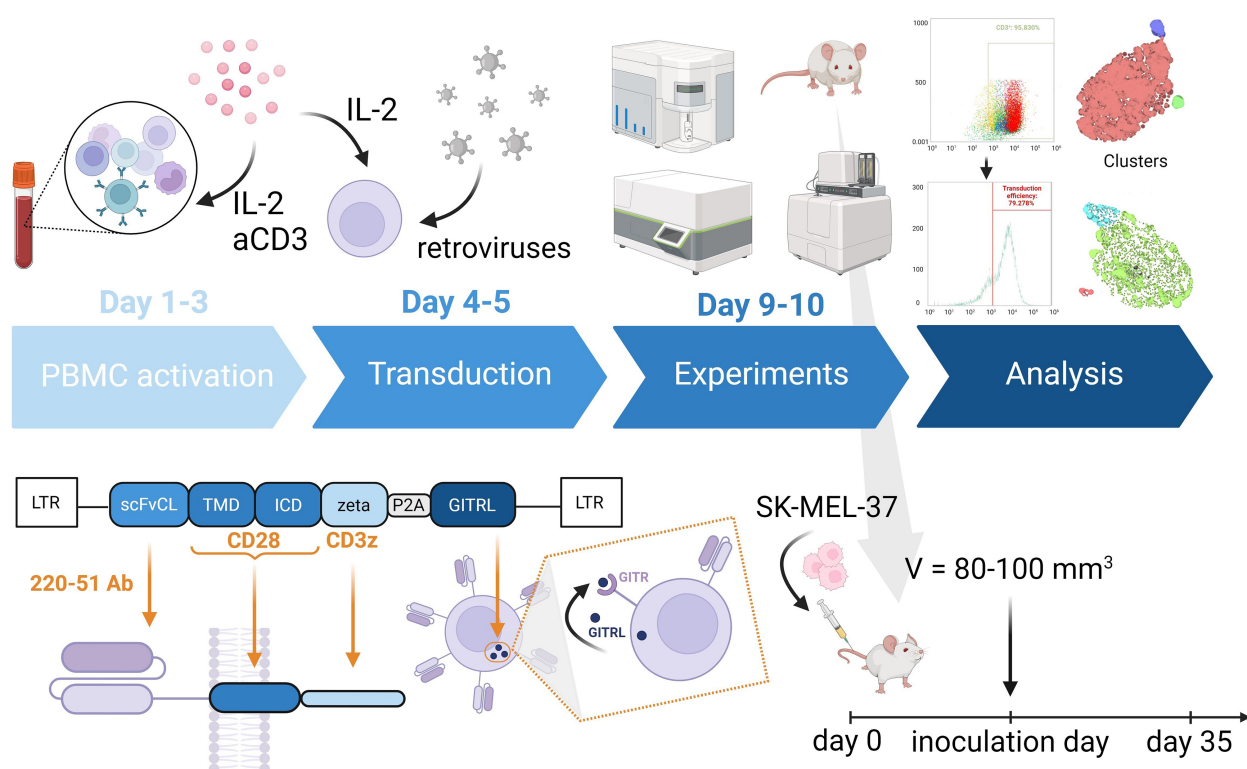


Fig. 1. Schematic representation showing the structure of the pGD2 transfer MMLV plasmid, and the *in vitro* and *in vivo* experiments. The CAR construct includes GD2-specific scFv from a modified mAb 220-51, as well as the human signaling endodomains CD28 (transmembrane and intracellular domain) and ξ -chain. GD2.CAR T cells express GITRL, which affects cells through autocrine or paracrine stimulation. CAR, chimeric antigen receptor; GD2, disialoganglioside; MMLV, Moloney murine leukemia virus; IL-2, interleukin-2. Created with [Biorender.com](https://www.biorender.com).

T551 medium (Cat. #WK551s, Takara Bio, Kyoto, Japan) supplemented with 300 U/mL interleukin-2 (IL-2) (Cat. #011022, Roncoleukin, Biotech, Saint Petersburg, Russia) and 0.6% group AB human serum. Half of the medium was replaced with fresh medium on days 2 and 3 supplemented with 300 U/mL IL-2. For retroviral transduction, retrovirus was diluted in PBS with 2% human serum albumin (Cat. #T160516, Microgen, Tomsk, Russia) and 5% glucose-citrate buffer, then added to RetroNectin-coated 24-well plates (25 μ g/mL RetroNectin). Plates were centrifuged at 32 °C and 2000 \times g for 2 h (Jouan MR 23i, Saint-Herblain, Nantes, France). After removing supernatant and washing twice with PBS containing 2% albumin, the activated PBMCs ($1.5\text{--}2 \times 10^5$ cells/well) were transduced with CAR for 10 min under centrifugation at 1000 \times g at 32 °C. The next day, these cells were transduced a second time. After 6–8 h, cells were transferred to 6-well plates (TPP, Trasadingen, Schaffhausen, Switzerland) with GT-T551 medium and 300 U/mL IL-2, and cultured at 37 °C and 5% CO₂. Transduced T cells were collected on days 9–10 for analysis (transduction efficiency and phenotyping), and used for *in vitro* cytotoxicity assays or *in vivo* experiments on day 11. To validate the generated CAR T cells, the identity of these cells was confirmed by flow cytometry (assessing T lymphocyte markers [CD3, CD4, and CD8] and

GD2-specific CAR) and light microscopy (assessing characteristic lymphocyte morphology: small size [7–10 μ m in diameter], high nuclear-to-cytoplasmic ratio, round nucleus, scant cytoplasm).

2.5 *In Vitro* Co-Culture Experiments

Tumor cells (SK-MEL-37, S6, and V9) were seeded at $4\text{--}5 \times 10^3$ cells/well in 96-well plates (TPP, Trasadingen, Schaffhausen, Switzerland) one day before co-culture with transduced or non-transduced T cells (effector to target ratio of 5:1) in fresh RPMI-1640 medium without exogenous cytokines. After 4–6 h of co-culture, T cells were collected for flow cytometry analysis of antigen-dependent activation and cytotoxicity markers. After 48 h co-culture of transduced or non-transduced T cells with GD2-positive SK-MEL-37 tumor cells, supernatants were collected and frozen for subsequent cytokine measurements. Cytotoxicity was assessed by measuring lactate dehydrogenase (LDH) activity in the conditioned medium of transduced T cells and tumor lines SK-MEL-37, S6, and V9 after 6–8 h.

2.6 Flow Cytometry and Transduction Efficiency

Flow cytometric analysis was performed using the following monoclonal antibodies (all from Biolegend, San Diego, CA, USA): CD3 (clone HIT3a), CD4 (clone

RPA-T4), CD8 (clone SK1), CD45RA (clone HI100), CD62L (clone DREG-56), CD137 (4-1BB) (clone 4B4-1), CD154 (CD40L) (clone 24-31), CD69 (clone FN50), CD178 (FasL) (clone NOK-1), CD107a (clone H4A3), CD366 (TIM-3) (clone F38-2E2), CD279 (PD-1) (clone EH12.2H7), and GD2 (clone 14G2a). These were conjugated with phycoerythrin (PE), PE-Cy7, peridinin-chlorophyll-protein complex (PerCP)-Cy5.5, allophycocyanin (APC)-Cy7, Alexa Fluor (AF) 647, AF488, AF700, Brilliant Violet (BV) 421, BV570, BV647, and BV711. Antibodies were used according to the manufacturer's recommendations, and FMO controls established negative gates. Transduction efficiency was assessed using biotin-SP-AffiniPure F(ab')₂-fragment-specific goat anti-mouse IgG (1:1000, Cat. #115-066-072, Jackson ImmunoResearch, West Grove, PA, USA) for the detection of GD2-CAR. Cells were stained by incubating with antibodies (1 to 1000 dilution) for 20 minutes at room temperature in the dark. After washing, streptavidin-PE (1 to 600 dilution) (1:600, Cat. #405203, Biolegend, San Diego, CA, USA), anti-CD3, and Zombie Aqua Dye (1:100, Cat. #423101, Biolegend, San Diego, CA, USA) were added to determine the population of CAR T cells and their viability. Stained cells were washed in PBS with 0.1% NaN₃ and analyzed on an Attune NxT flow cytometer. Non-transduced cells served as controls.

2.7 HSNE Dimensionality Reduction and Clustering Analysis

Flow cytometry data analysis was performed using a combination of software tools. Cells were gated using Attune NxT software (version 3.2.1, Thermo Fisher Scientific, Waltham, MA, USA) to exclude debris, doublets, and dead cells, and to identify CD3⁺ and transduced cells (**Supplementary Fig. 1**). The resulting .fcs files were converted to .csv format using custom Python (version 3.13, Wilmington, DE, USA) code via Jupyter Notebooks (version 6.5.4, Austin, TX, USA). Subsequently, the .csv files were *arcsinh*-transformed and *fdNorm*-normalized using an R script [21] and exported as .fcs files. HSNE dimensionality reduction was performed using the Cytosplore app [22] on cytotoxic and activation markers (CD4, CD8, CD40L, CD69, 107a, 4-1BB, and FasL), and T cell memory and exhaustion markers (CD8, CD45RA, CD62L, CD69, PD-1, and TIM-3). Subsequently, GraphPad Prism (version 9.4.1, GraphPad Prism Software, San Diego, CA, USA) was used to export cell frequencies per cluster and visualize them as box plots.

2.8 Cytokine Production Assay

Cytokine concentrations in supernatant were measured using the LEGENDplex™ Human CD8/NK Panel (13-plex) and Filter Plate Kit (Cat. #740267, Biolegend, San Diego, CA, USA) according to the manufacturer's recommendations. Cytokines were subsequently classified based on their respective concentration levels.

2.9 LDH Cytotoxicity Assay

Cytotoxicity was assessed by measuring LDH release in cell culture supernatants using a CytoTox 96 Non-Radioactive Cytotoxicity Assay (Cat. #G1780, Promega Corporation, Madison, WI, USA) according to the manufacturer's recommendations. This assay measures LDH activity via a 30-minute enzymatic reaction that converts tetrazolium salt INT into red formazan product. The absorbance of the resulting color was measured using a Varioskan plate reader (Thermo Fisher Scientific, Waltham, MA, USA). Color intensity correlated with the number of lysed cells.

2.10 Magnetic Separation of CAR T Cells

For gene expression analysis, transduced T cells were isolated using a two-step magnetic sorting procedure. First, cells were incubated with F(ab')₂-fragment-specific goat anti-mouse IgG antibodies for 20 minutes in cold Versene solution containing 0.5% bovine serum albumin, labeled with MojoSort™ Streptavidin Nanobeads (Cat. #480016, Biolegend, San Diego, CA, USA) at a ratio of 10 µL antibodies/beads per 10 × 10⁶ cells, and then positively selected using a MojoSort™ Magnet (Cat. #480019, Biolegend, San Diego, CA, USA). After resting for 16–17 h in culture medium supplemented with 300 U/mL IL-2, the purified T cells were co-cultured with GD2-positive SK-MEL-37 tumor cells at an effector-to-target ratio of 5:1 for 2 h to activate gene expression of the immune response. Finally, transduced T cells were sorted again by positive selection using MojoSort™ Human CD45 Nanobeads (Cat. #480029, Biolegend, San Diego, CA, USA) to ensure a pure CAR T cell population. Cell viability, assessed by trypan blue staining using a Countess 3 Automated Cell Counter (Thermo Fisher Scientific, Waltham, MA, USA), was consistently >92%.

2.11 RNA Extraction

Total RNA was extracted from 3–6 × 10⁵ cells using the Total RNA Purification Plus Kit (Cat. #48400, Norgen Biotek, Thorold, ON, Canada) according to the manufacturer's recommendations. RNA concentration and quality were assessed using a Nanodrop 2000 spectrophotometer (Thermo Fisher Scientific, Waltham, MA, USA). Total RNA was frozen at –80 °C until further analysis.

2.12 NanoString Gene Expression Analysis

Gene expression analysis was performed using the NanoString nCounter SPRINT Profiler system with 100 ng of total RNA per sample (n = 6). The nCounter Human Immunology v2 panel, comprising 579 genes (Cat. #XT-CSO-HIM2-12, NanoString, Seattle, WA, USA), was used to analyze RNA samples on the NanoString Sprint instrument (NanoString, Seattle, WA, USA). Samples were hybridized according to the manufacturer's recommendations. Normalization and quality control were performed using nSolver 4, incorporating synthetic positive controls and the

15 housekeeping genes included in the panel. To remove non-expressing genes, a background threshold was applied to the normalized data, defined as: (mean of all NEG controls) + $2 \times$ (SD of all NEG controls) + (mean of the POS_E controls). Gene Set Enrichment Analysis was performed using GSEAPy [23].

2.13 In Vivo Experiment

To determine the anti-tumor efficacy of transduced T cells *in vivo*, 8-week-old male or female non-obese diabetic (NOD)/Rag1-null/Il2r γ -null (NRG) mice (NOD.Cg-Rag^{1tm1Mom} Il2r γ ^{tm1Wjl}/SzJcgn) (Center for Collective Usage SPF-vivarium, Institute of Cytology and Genetics, Siberian Branch of the Russian Academy of Sciences, Novosibirsk, Russia) were injected subcutaneously in the right scapula region with 5×10^6 SK-MEL-37 cells in 100 μ L culture medium. When tumors reached approximately 80–100 mm³, mice were divided into a control group (intratumoral injection of 8×10^6 activated non-transduced T cells in 100 μ L RPMI-1640 medium), an experimental group (intratumoral injection of 8×10^6 GD2.CAR T cells in 100 μ L RPMI-1640 medium), and an untreated group ($n = 8$ per group). Tumor growth was monitored every 2–3 days using calipers, and tumor volume was calculated as: volume = $0.52 \times \text{width}^2 \times \text{length}$. Mice were maintained under specific-pathogen-free (SPF) conditions with a 12-h light-dark cycle, and their health monitored regularly. Euthanasia was performed using CO₂ overdose (3 L/min fill rate, resulting in approximately 30% CO₂ concentration) followed by cervical dislocation, as indicated by clinical signs of disease (e.g., not eating, lack of activity, abnormal grooming behavior, hunched posture), excessive weight loss (>15% over one week), or tumor size reaching approximately 2000 mm³. The research was conducted at the Center for Genetic Resources of Laboratory Animals, Institute of Cytology and Genetics, Siberian Branch of the Russian Academy of Sciences, and approved by the local ethics committee of the Research Institute of Fundamental and Clinical Immunology (protocol #139 on May 30, 2022) as per the European Community Directive (86/609/EEC) and humane treatment standards.

2.14 Statistical Analysis

Data are presented as frequencies, percentages, or mean \pm SEM. The Shapiro–Wilk test was used to assess normality. Statistical significance between transduced and non-transduced cells was determined using GraphPad Prism 9.4.1, with one-way or two-way ANOVA followed by *t*-test, Dunnett's test, or Tukey's test. LDH cytotoxicity was analyzed using one-way ANOVA with Dunnett's test for multiple comparisons. Differential gene expression and cytokine production were analyzed using multiple *t*-tests with FDR-adjusted *p*-values < 0.05. Animal experiments were analyzed using two-way ANOVA with Tukey's test for multiple comparisons. All *p*-values and *n* numbers are reported in the figure legends. A *p*-value < 0.05 was considered statistically significant.

3. Results

3.1 Detection of GD2 Expression in Melanoma, and GD2.CAR T Cell Transduction Efficiency

Three human melanoma cell lines (SK-MEL-37, S6, and V9) were analyzed for surface expression of GD2 by flow cytometry using mAb 14.G2a. The SK-MEL-37 and S6 cell lines showed high GD2 expression (89.4% and 85.1%, respectively). The V9 cell line was used as a negative control due to its low GD2 expression (2.3%) and antigen density on the cell surface.

The second-generation CAR construct containing GD2-specific scFv from a modified mAb 220-51 [19] and human signaling endodomains CD28 and CD3 ζ , was transduced into activated T lymphocytes using retroviral vectors (Fig. 1). Seven days after transduction, we assessed GD2-specific CAR expression by flow cytometry and observed $68.2 \pm 3.5\%$ ($n = 6$, mean \pm SEM) GD2.CAR⁺ T cells. In order to provide strong co-stimulation and a potential synergistic effect of CD28 signaling in T cell activation [20], T lymphocytes were also genetically engineered to co-express the GITRL with CAR, as demonstrated in a recent study [19].

3.2 Subsets of GD2.CAR T Cells and Markers of Cell Exhaustion After Transduction

To further evaluate the signature of GD2.CAR T cell memory subpopulation changes, flow cytometry and HSNE analysis were used to assess marker expression according to T cell memory subsets immediately after transduction and before co-culture with the tumor cells. CAR T cells were classified into four differentiation subsets based on CD45RA and CD62L expression: naive/stem memory T cells (Tn/scm, CD62L⁺CD45RA⁺), central memory T cells (Tcm, CD62L⁺CD45RA⁻), effector memory T cells (Tem, CD62L⁻CD45RA⁻), and late effector memory T cells (Temra, CD62L⁻CD45RA⁺) [24]. HSNE analysis (Fig. 2) revealed the CD8⁺ GD2.CAR T cell population was mainly composed of Tn/scm cells, with only small percentages of Tcm and Temra cells observed (Supplementary Fig. 2).

Expression of the cell exhaustion markers programmed cell death protein 1 (PD-1) and T-cell immunoglobulin and mucin domain-containing protein 3 (TIM-3) was also evaluated. In general, the GD2.CAR T cell population did not show signs of exhaustion. However, a correlation was observed between the expression of CD45RA and CD62L markers and the expression of TIM-3 and PD-1 markers. The expression of cell exhaustion markers gradually increased as the cells differentiate into Tcm cells, and decreased in Temra cells (Fig. 2). It was previously reported that the increase in CD69 level is likely a manifestation of the basal level of activation by CAR-mediated tonic signaling [25]. Our transduction protocol resulted in a population of CD69⁻ CAR T cells, indicating the potential absence of tonic signaling. Meanwhile, only a low proportion of CD69⁺ T cells was observed (Fig. 2).

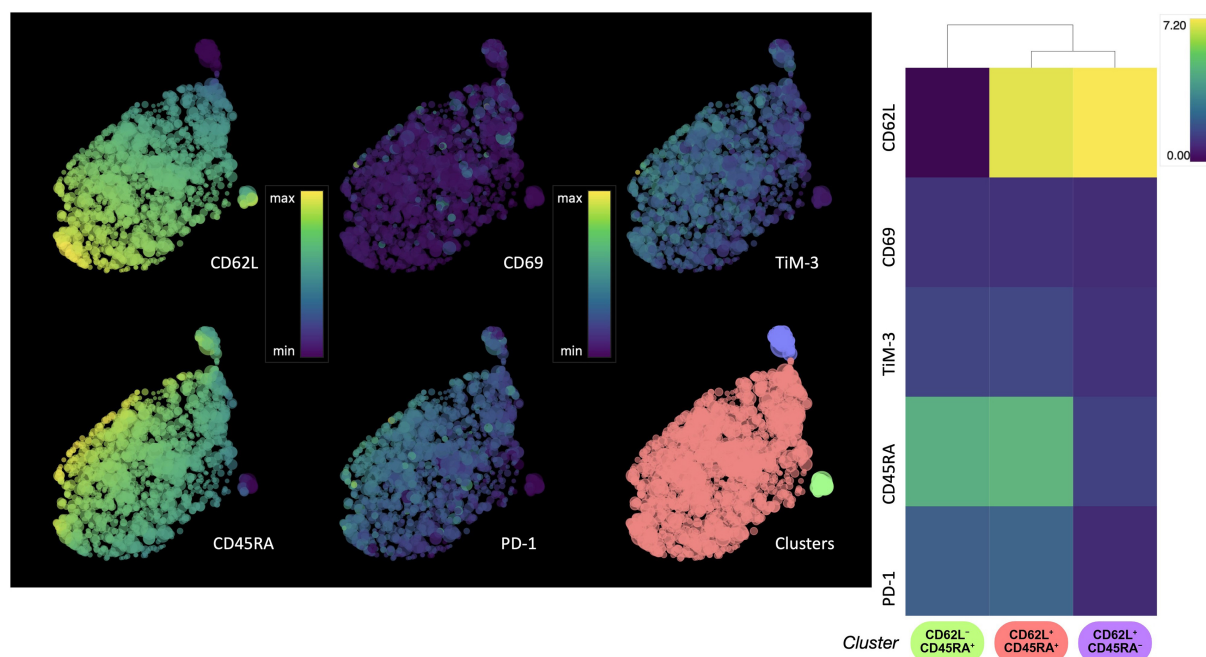


Fig. 2. HSNE analysis of the expression of T cell memory and activation/exhaustion markers in CD8⁺ GD2.CAR T cells. Single-cell level HSNE dot plots show the expression of T cell memory (CD62L, CD45RA) and activation/exhaustion (PD-1, TIM-3) markers by CD8⁺ GD2.CAR T cells after transduction. The color scale represents the level of expression for *arcsinh* transformation phenotypic markers, where violet color indicates low expression and yellow color indicates high expression. The clusters are color-coded based on the heat map (n = 5). HSNE, hierarchical stochastic neighbor embedding; PD-1, programmed cell death protein 1; TIM-3, T-cell immunoglobulin and mucin domain-containing protein 3.

Furthermore, the CD69 marker is expressed only when an effector cell recognizes an antigen [26].

3.3 Transcriptome Profile of GD2.CAR T Cells Associated With the Tn/scm Phenotype

To investigate how retroviral transduction affects the expression of genes related to phenotypic signatures (Fig. 3), we used NanoString technology to compare the transcriptome profiles of transduced and non-transduced cells. After transduction, GD2.CAR T cells showed upregulation of genes associated with the CD8 Tn cell differentiation signature, including *CD8A*, *CD8B*, *SELL*, *IL7R*, *CD45RA* [27], and *IL2RG* [28], as well as genes associated with the CD8 Tscm/cm cell differentiation signature, such as *FAS* and *CD45RO* [27]. Upregulation of the *CD40LG* gene, which is canonically expressed on CD4⁺ T cells, was also observed in CAR⁺ cells [29]. In contrast, transduced cells showed downregulation of CD4 Treg-associated genes, including *CD4*, *FOXP3*, *IL2RA*, and *CTLA4-TM* [27]. It is worth noting that retroviral transduction had an impact on T cell proliferation, whereas anti-CD3-primed non-transduced cells showed upregulation of genes related to T cell activation, such as *TNFRSF4* and *TNFRSF9* [30]. Furthermore, GD2.CAR T cells showed increased expression of the *HAVCR2* gene within the T cell exhaustion signature, whereas non-transduced cells showed increased expression of the *LAG3* gene.

3.4 Immune Characteristics of GD2.CAR T Cell Transcriptome Profile in the Early Stages of Interaction With GD2-Positive Melanoma Cells

Using NanoString technology, we performed differential gene analysis of GD2.CAR T cells before and after co-culture with SK-MEL-37 cells. Because our aim was to examine changes in gene expression linked to the immune response before and after co-culture with tumor cells, we selected the Human Immunology v2 panel for this study. CAR⁺ cells were first magnetically sorted from the general cell population and then stimulated with IL-2 for 16–17 h. GD2.CAR T cells were then cultured with tumor cells for 2 h to activate key genes that regulate the immune response. These cells were then separated from GD2-positive SK-MEL-37 cells using CD45-positive magnetic sorting to remove any contamination with tumor cells.

Although the interaction between GD2.CAR T cells and tumor cells was short, alterations were detected in several genes (**Supplementary Table 1**) encoding co-signaling molecules, cytokines, and chemokines that affect the immune response (Fig. 4A).

Signatures for chemokines (*CCL2*, *CCL20*, *CCL3*, *CCL4*, *CXCL1*, *CXCL10*, *CXCL11*, and *CXCL2*), cytokines and their receptors (*CSF1*, *CSF2*, *IL13*, *IL13RA1*, *IL1A*, *IL1B*, *IL1RAP*, *IL6*, *IL8*, and *IFNG*) were found after co-culture with the tumor cell line. In contrast, a decrease in the expression of chemokine receptor genes (*CCR1*, *CCR2*,

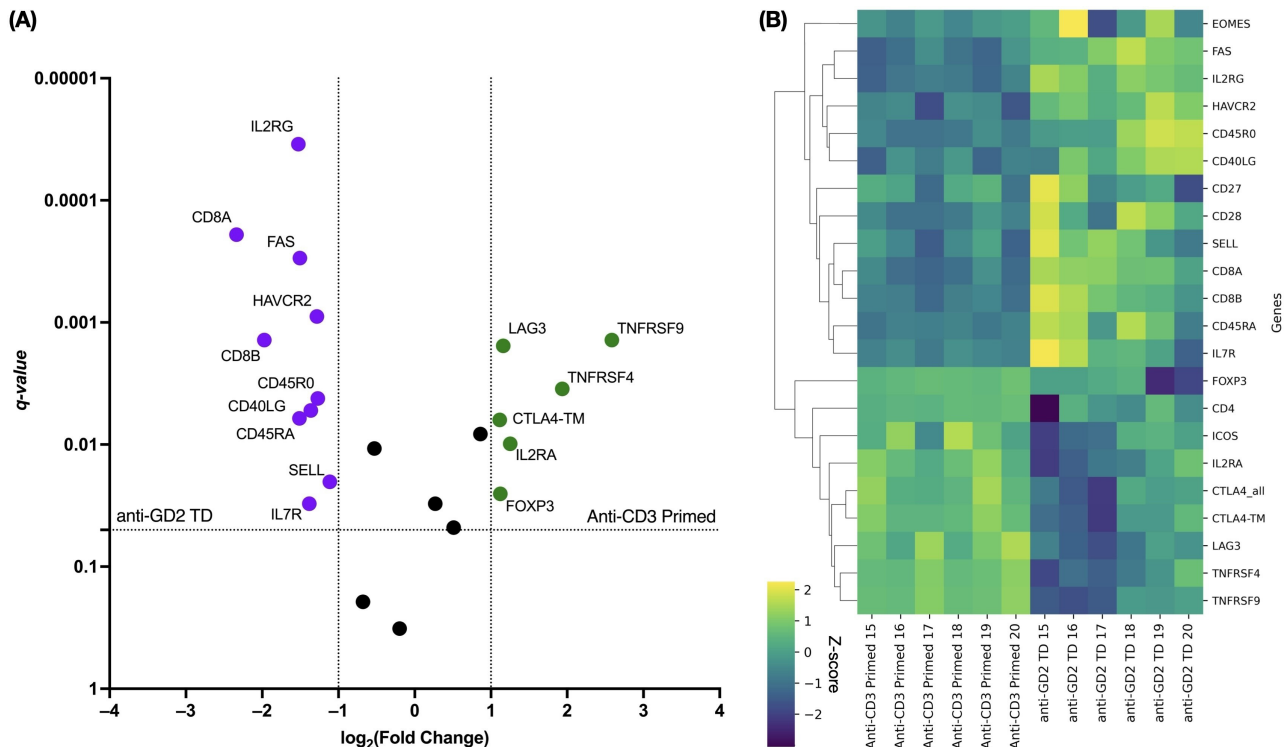


Fig. 3. Differential gene expression in transduced versus non-transduced T cells related to the Tn/scm phenotype. (A) The volcano plot shows significantly up- and down-regulated genes. Violet color indicates up-regulated genes in transduced cells, while green color indicates down-regulated genes in non-transduced cells. q -values < 0.005 (dotted line on the y -axis) and \log_2 (fold-change) > 0.847 or \log_2 (fold-change) < -0.847 (dotted lines on the x -axis) were considered to be significant. (B) The heat map indicates z-score normalized gene expression of transduced and non-transduced T cells. The color scale represents the level of expression for each gene (blue color indicates low expression, yellow color indicates high expression).

CCR5, *CCR7*, *CCRL2*, *CX3CR1*, *CXCR3*, *CXCR4*, and *CXCR6*) was observed, as well as that of cytokine receptors and their component genes (*IL10RA*, *IL12RB1*, *IL21R*, *IL2RG*, *IL4R*, and *IL7R*). We also observed a decrease in the expression of genes associated with the Tem cell differentiation signature, including *CCR7*, *CD27*, *CD28*, *CD45RA*, *CD45RB*, *CX3CR1*, *IL7R*, *LEF1*, and *TCF7* [27]. Furthermore, increased expression of the *CTNNB1* [31,32] and *BCL6* [33] genes and decreased expression of the *LAIR1* [34] and *SELPLG* [35] genes are also signatures of Tem cell differentiation. Regarding the effector function of T cells, increased expression of genes associated with activation was observed, including *TNFRSF9* [30] and MHC class II genes (*HLA-DMA*, *HLA-DMB*, *HLA-DPA1*, *HLA-DPB1*, *HLA-DQA1*, *HLA-DRA*, *HLA-DRB1*, and *HLA-DRB3*), as well as genes associated with migration (*IL6*, *IL6ST*, *SELE*, and *ICAM1*) [36]. We also observed upregulation of *TRAF1* gene expression, which is involved in downstream signaling of 4-1BB [37] or GITR [38]. Upregulation of *EGR2* gene expression was also observed, which promotes differentiation toward Tem cells and regulation of the exhausted transcriptional state [39], as well as improved survival and proliferation [40]. However, the expression of genes encoding effector molecules (*GZMA*, *GZMK*, and *PRF1*) and sig-

naling molecules (*LCK* and *ZAP70*) essential for the initiation of TCR signaling were downregulated [41]. Notably, after co-culture of GD2.CAR T cells with tumor cells, decreases were observed in signatures associated with T cell dysfunction, including expression of the *HAVCR2*, *CISH* [42,43], *CD244* and *SLAMF7* [44] genes, as well as T cell death genes (*BAX*, *BCL2*, *CASP1*, and *CASP8*) [45,46].

The up-regulated genes (Supplementary Table 2) were enriched by gene set enrichment analysis (GSEA) [23] using ontology biological process terms. GSEA analysis revealed that the top three pathways were associated with the cytokine-mediated signaling pathway, cellular response to interferon-gamma, and interferon-gamma-mediated signaling pathways (Fig. 4B). In contrast, genes associated with T cell proliferation and cytokine production were not significantly expressed during early stages of the CAR T cell-tumor interaction.

3.5 GD2.CAR T Cells are Predominantly CD8⁺ T Cells With a Cytotoxic Phenotype

To investigate the potential application of CAR T cells as effector cells against melanoma, we evaluated the expression of surface activation and cytotoxicity markers (CD69, 4-1BB or CD137, CD107a, FasL, and CD40L) following 4–6 h of co-culture with GD2-positive

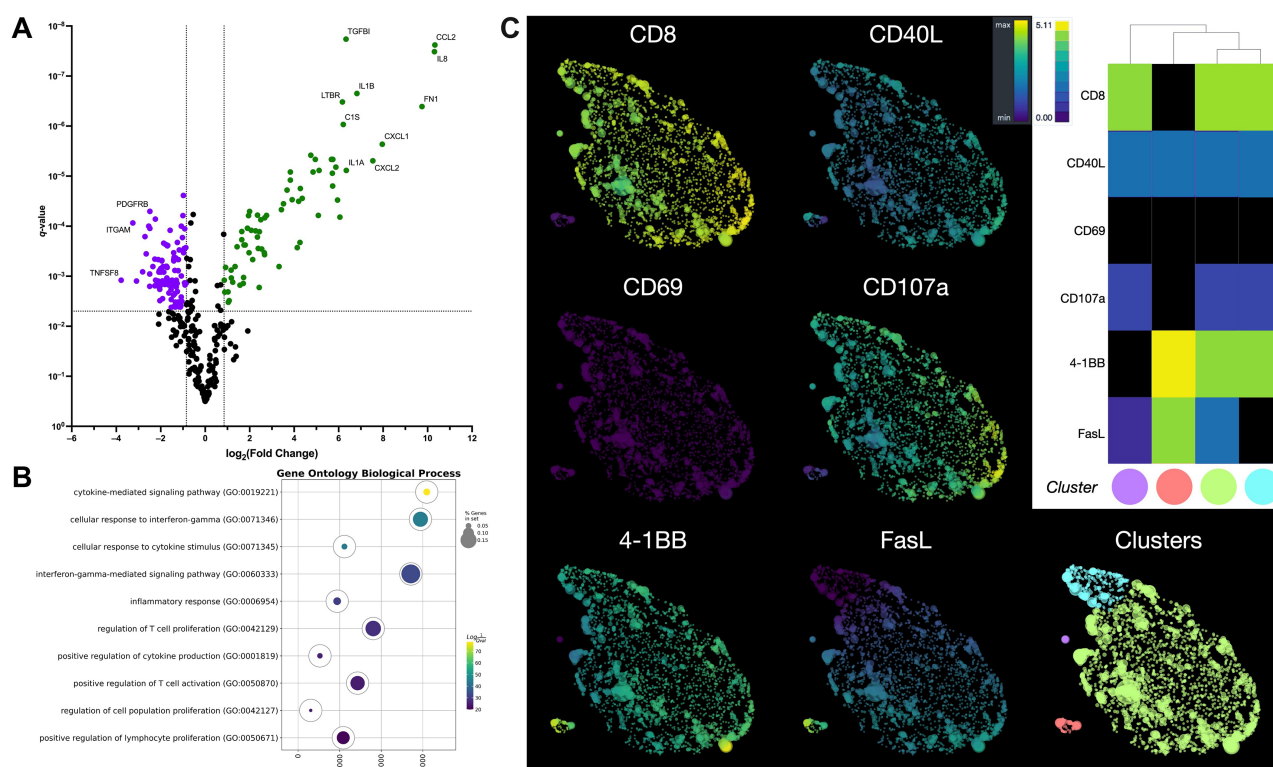


Fig. 4. Comprehensive analysis of gene expression, signaling, and phenotype in GD2.CAR T cells following co-culture with a melanoma cell line. (A) The volcano plot shows differentially expressed genes in GD2.CAR T cells before and after co-culture with SK-MEL-37 cells. Green color indicates up-regulated genes, while violet color indicates down-regulated genes. q -values < 0.005 (dotted line on the y-axis) and $\log_2(\text{fold-change}) > 0.847$ or $\log_2(\text{fold-change}) < -0.847$ (dotted lines on the x-axis) were considered to be significant. (B) A GSEA bubble plots show Gene Ontology Biological Process terms that were significantly enriched in up-regulated genes in the GD2.CAR T cells. The bubble size indicates the percentage of genes involved in the respective biological process or pathway. The color represents the corrected p -value of the enriched pathway (q -values < 0.000001). The top pathways involved in biological processes are shown on the x-axis. (C) Single-cell level HSNE dot plots show the expression of activation and cytotoxicity markers (CD69, 4-1BB, CD107a, FasL, and CD40L) by CD8⁺ GD2.CAR T cells after 4–6 h of co-culture with SK-MEL-37 cells. The color scale represents the level of expression for *arcsinh* transformation cytotoxic markers, where violet color indicates low expression and yellow color indicates high expression. The clusters are color-coded based on the heat map (n = 6).

tumor cell lines. This duration is sufficient to induce expression of the markers. Using a panel of antibodies, we analyzed the flow cytometry data from the GD2.CAR T cells using HSNE dimensionality reduction after *arcsinh* transformation with automated cofactors. Data were normalized using *fdaNorm* to correct for batch effects and ensure data integrity. HSNE analysis identified four GD2.CAR T cell subpopulations (Fig. 4C). The predominant population was CD8⁺CD40L⁺CD69⁺CD107a⁺4-1BB⁺FasL⁺ T cells, suggesting cytotoxic function (Supplementary Fig. 3). Smaller populations of CD8⁺CD40L⁺CD69⁺CD107a⁺4-1BB⁺FasL⁺ and CD4⁺CD40L⁺CD69⁺CD107a⁺4-1BB⁺FasL⁺ T cells with similar proportions were also observed, as well as a minor population of CD8⁺CD40L⁺CD69⁺CD107a⁺4-1BB⁺FasL⁺ T cells (Supplementary Fig. 3).

3.6 GD2.CAR T Cells Show Specific and Efficient Cytotoxicity Against GD2-Positive Melanoma Cells In Vitro

The LDH release assay was employed to assess the cytotoxic activity of GD2.CAR T cells against melanoma tumor cell lines expressing the GD2 antigen. CAR T cells were co-cultured at an effector-to-target ratio of 5:1 for 6–8 h with tumor cells that expressed GD2 (SK-MEL-37 and S6), or did not express GD2 (V9) (Fig. 5). This ratio and co-culture duration were based on the manufacturer's protocol and optimized for reliable results in the LDH release assay. Significant differences in GD2-specific anti-tumor cytotoxicity, as measured by LDH release, were observed after co-culture with the GD2-expressing SK-MEL-37 and S6 tumor cell lines. Importantly, no significant differences in cytotoxicity were observed between the SK-MEL-37 and S6 cell lines. These results demonstrate the efficacy and specificity of GD2.CAR-T cells in targeting GD2-expressing melanoma cells.

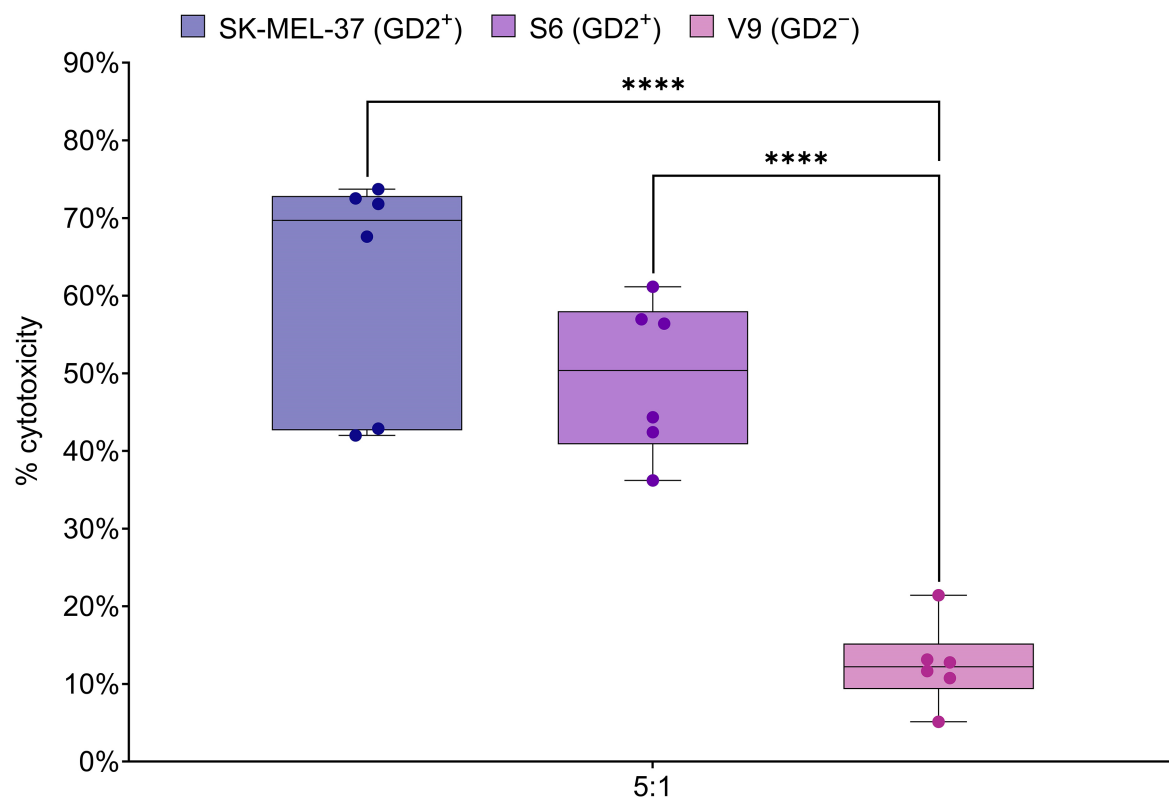


Fig. 5. GD2.CAR T cell cytotoxicity against melanoma cell lines. Box plots show LDH release, a measure of cytotoxicity, following 6–8 h co-culture of GD2.CAR T cells with GD2-positive SK-MEL-37 (89.4% GD2 expression), S6 (85.1% GD2 expression) and GD2-negative V9 (2.3% GD2 expression) melanoma cell lines at a 5:1 effector-to-target ratio (n = 6). Asterisks indicate significant *p*-values as follows: *****p* < 0.0001, one-way ANOVA with Dunnett's test for multiple comparisons. These results indicate the strong cytotoxic activity of CAR T cells against GD2-positive cell lines. LDH, lactate dehydrogenase; ANOVA, analysis of variance.

3.7 GD2.CAR T Cells Secrete Cytokines in Response to Co-Culture With GD2-Positive Melanoma Cells

Cytokine release from transduced and non-transduced T cells was assessed 48 h after contact with a GD2⁺ target at an effector-to-target ratio of 5:1. The LEGENDplex™ Human CD8/NK panel was used to simultaneously analyze cytokines, including IL-2, IL-6, and IL-17, and effector molecules, including granzyme A, granzyme B, granzyme C, perforin, and sFasL, in the cell co-culture supernatants. Compared to non-transduced T cells, GD2.CAR T cells tended to secrete more pro-inflammatory cytokines and effector molecules (Fig. 6). No statistically significant differences between non-transduced cells and GD2.CAR T cells were observed for the levels of perforin, granzyme B, granzyme C, IL-2, and IL-6 in the culture medium. However, significant increases were observed in the levels of granzymes A/B, IFN- γ , and sFasL secreted by GD2.CAR T cells. IL-4, IL-10, and sFas were not detected in the supernatants of GD2.CAR and non-transduced T cells.

3.8 GD2.CAR T Cells Inhibit the Growth of GD2-Positive Melanoma in a Xenograft Model

We next evaluated the antitumor efficacy of generated GD2.CAR T cells against GD2-positive tumors in a

xenograft model by inoculating SK-MEL-37 cells (5×10^6 cells per mouse) into NRG mice via subcutaneous injection. When the tumor volume reached 80–100 mm³, tumor-bearing mice were randomized to receive a single intratumoral injection of either 8×10^6 GD2.CAR T cells or 8×10^6 anti-CD3-primed non-transduced T cells. Tumor growth was monitored by caliper measurements. Local intratumoral injection was chosen as the route for T cell administration based on the efficacy demonstrated in a pre-clinical study with locally injected CAR T cells [13]. Three weeks into the experiment, the tumor volume increased rapidly in untreated mice and in mice that received non-transduced T cells (Fig. 7). At 35 days after intratumoral administration of GD2.CAR T cells, a significant reduction in tumor size was observed compared to both the control group and the intact group.

4. Discussion

In this study, we comprehensively analyzed the phenotypic and functional characteristics of GD2.CAR T cells containing CD28 and CD3 ζ endodomains, alongside GITRL secretion. The differentiation state of CAR T cells is critical in determining the efficacy of tumor therapy [47]. In particular, the immunophenotypes of T_n, T_{cm} and T_{em}

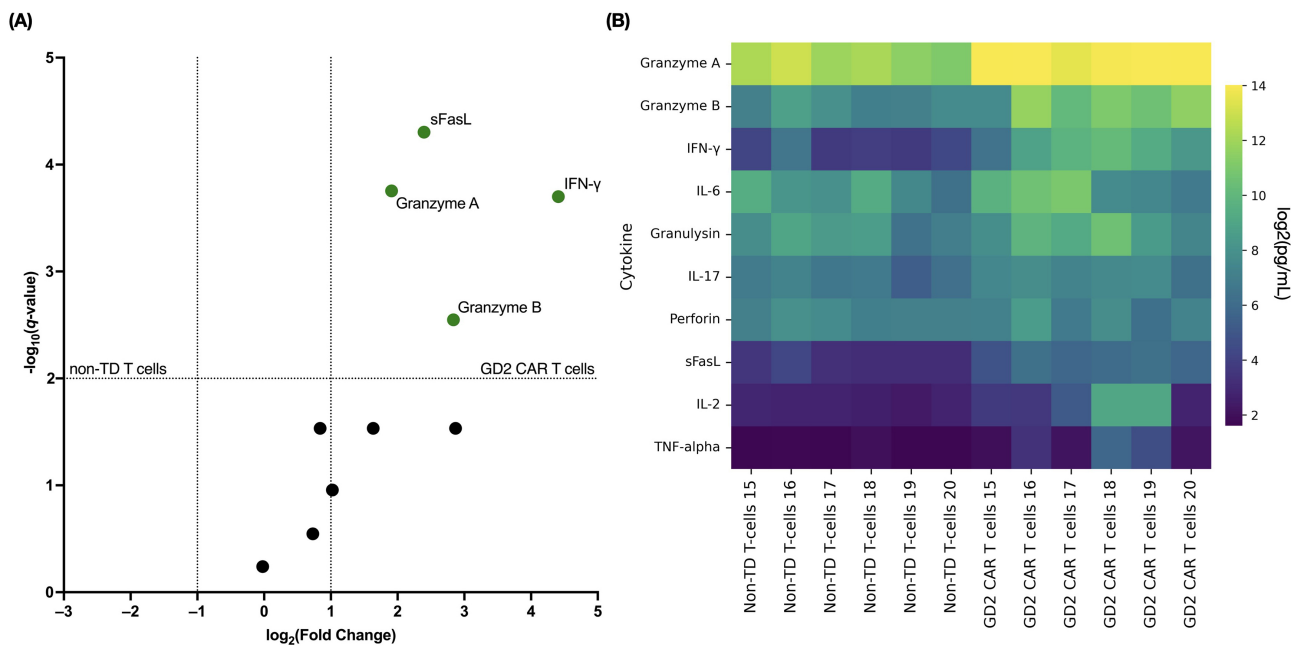


Fig. 6. Cytokine response of GD2.CAR T cells to co-culture with SK-MEL-37. (A) The volcano plot shows fold-changes in cytokine levels in co-culture supernatants of GD2.CAR T cells (green dots indicate significance) with SK-MEL-37 cells (compared to non-transduced T cells). The x-axis values represent log₂ (fold-change), and the y-axis values represent -log₁₀ of *q*-values. The *q*-values indicate FDR-adjusted *p*-values for multiple *t*-tests. The upper right quadrant indicates statistically significant results (*q*-value < 0.05). (B) The heat map shows the average log FCs of cytokine levels (pg/mL) for both transduced and non-transduced cells. The color scale represents cytokine levels (blue color indicates low concentration, yellow color indicates high concentration).

cells are preferred for adaptive therapy because of their antitumor efficacy, survival and proliferation [48]. Our optimized protocol resulted in GD2.CAR T cells comprised mainly of naive CD62L⁺CD45RA⁺ T cells. Transcriptional analysis revealed that retroviral transduction affects the proliferative potential of CAR⁺ cells, as confirmed by the frequency of the Tn cell population. The majority of CAR⁺ cells belonged to the subpopulation of CD8⁺ T cells expressing CD107a, FasL, 4-1BB, and CD40L markers, indicating activation and cytotoxicity. In addition, the GD2.CAR T cell population contains a small percentage of CD4⁺ T cells that express effector molecules, such as CD40L, 4-1BB, and FasL. Recent research suggests that CD4⁺ CAR T cells can enhance antitumor activity and maintain the immune response against tumors [49,50]. After transduction, the expression of genes associated with the regulation of Treg cells is downregulated. Therefore, the generated population of CD4⁺ CAR T cells may contribute to antitumor immunity. The FasL marker showed higher expression compared to the CD107a marker, while the *PRF1* gene was downregulated. No statistically significant differences in perforin secretion were found between transduced and non-transduced T cells. Nevertheless, due to synergistic or additive effects between degranulation and ligand-based lytic pathways, FasL has been shown to promote lytic activity even when degranulation is poor or difficult in CAR T cells [51]. Furthermore, we did not observe expression of the early activation marker CD69 on

GD2.CAR T cells. CD69 protein expression can be detected 2–3 h after activation, whereas transcriptional expression of the *CD69* gene decreases after 4–6 h [26]. We propose that an off-the-shelf, activated cell product of CAR T cells would have either a low level of CD69 expression or none at all. In addition, the generated GD2.CAR T cells did not express the CD69 marker after transduction, suggesting a lack of basal activation by CAR-mediated tonic signaling [25]. Moreover, a recent study has shown that CD69⁺ CAR T cells have increased proliferation and downregulated expression of surface markers associated with dysfunction [52].

The CD137 receptor serves as a T cell activation marker and is expressed on the cell surface after CD3 or CD28 stimulation [53]. This results in the activation of intracellular signaling through TRAF-mediated activation of NF-κB and MAPK, leading to increased cell survival and enhanced effector functions. We found that early co-culture of GD2.CAR T cells with tumor cells results in up-regulation of *TRAF1* and *TNFRSF9* gene expression, suggesting that antigenic stimulation of CARs or the GITR-GITRL interaction [38,54] may enhance signaling. The GITR-GITRL interaction has a dual effect on the CD3⁺ T cell population, as it can promote the generation of both Treg cells and cytotoxic CD8⁺ T cells [55]. Nevertheless, we observed downregulation of *TGFB1* and *TGFB1* gene expression, which control development of the Treg cell population [56,57]. Therefore, we suggest that GITRL pro-

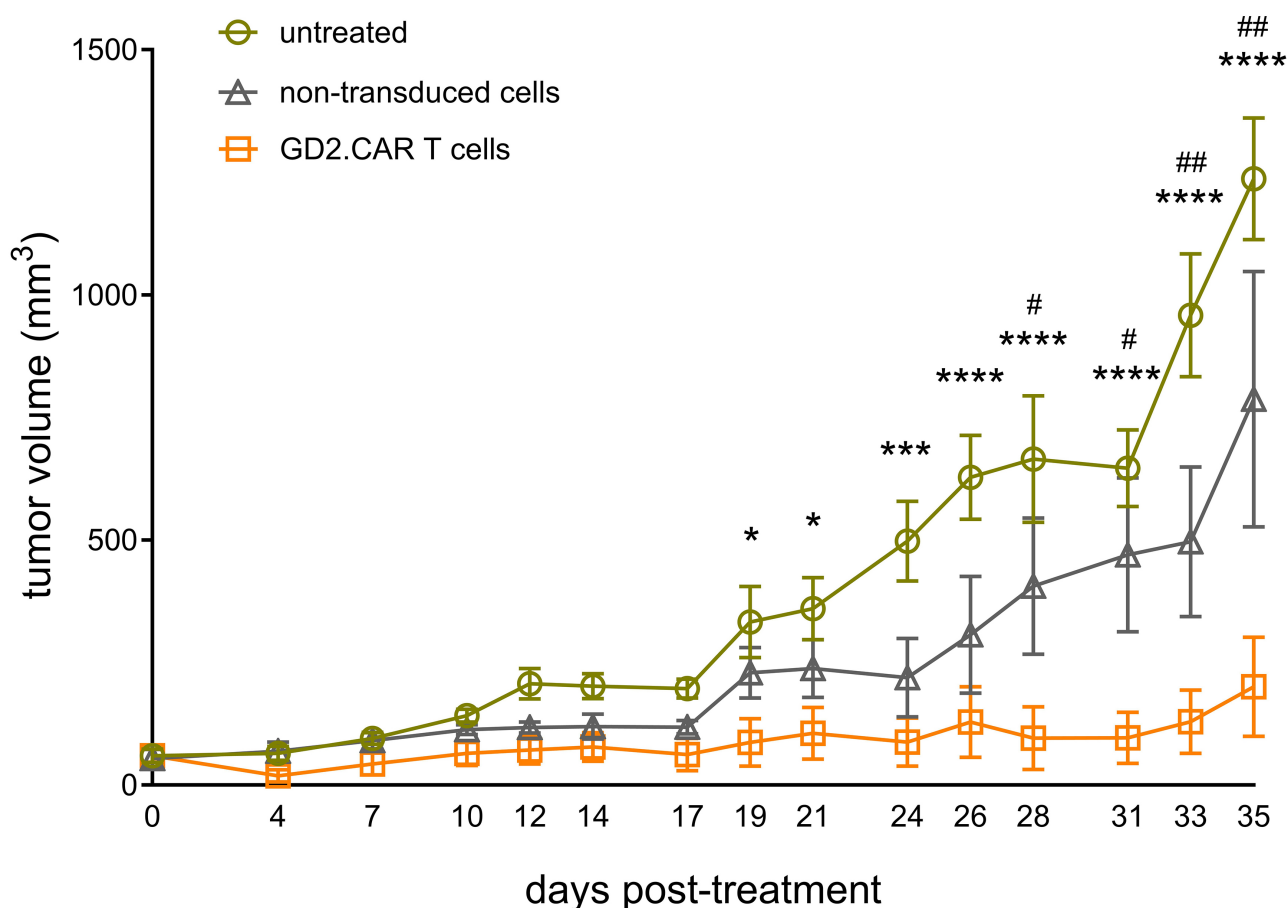


Fig. 7. Antitumor efficacy of GD2.CAR T cells *in vivo*. SK-MEL-37 cells were subcutaneously inoculated into NRG mice ($n = 24$) at a dose of 5×10^6 cells per mouse. Once the tumor size reached 80–100 mm³, non-transduced T cells were injected into the control group, while GD2.CAR T cells were injected into the experimental group at a dose of 8×10^6 cells per mouse. Results are presented as the mean tumor volume (mm³) \pm SEM. Asterisks indicate significant differences between GD2.CAR T cell-treated and untreated groups, with p -values indicated as follows: * $p < 0.05$, *** $p < 0.001$, **** $p < 0.0001$; grids indicate significant differences between GD2.CAR T cell and non-transduced T cell-treated groups, with p -values indicated as follows: # $p < 0.05$, ## $p < 0.0001$, two-way ANOVA with Tukey's test for multiple comparisons. NRG, non-obese diabetic (NOD)/Rag1-null/Il2r γ -null (NOD.Cg-Rag^{tm1Mom} Il2r^{tm1Wjl}/SzJcgn); SEM, standard error of the mean.

motes the development of effector CD8⁺ T cells, as evidenced by the increased expression and secretion of inflammatory cytokines, alongside the absence of detectable IL-10. Furthermore, previous research has shown that forced expression of GITRL in CAR T cells resulted in increased IFN- γ production [19]. We also observed upregulation of *IFNG* gene expression and activation of IFN- γ -mediated signaling pathways, which may indicate a GITR-GITRL interaction within the CAR T cell population. *ZAP70* and *LCK* genes, which encode TCR signaling proteins [58], were also found to be downregulated. Since CAR T cells have a modified TCR, the expression of these genes may differ from the canonical TCR pathway compared to non-transduced T cells [59].

It is well known that cytotoxic CD8⁺ CAR T cells exert antitumor effects through several underlying mechanisms, including the perforin-granzyme axis, the Fas-FasL

axis, and cytokine secretion [51]. The GD2.CAR T cells we generated have significant cytotoxic efficacy and the ability to express FasL and the degranulation marker CD107a on their cell surface, as well as the secretion of effector molecules such as granzyme A/B, the pro-inflammatory cytokine IFN- γ , and the soluble form of FasL. The production of IL-6 and IFN- γ by CAR T cells is a double-edged sword, as these cytokines contribute significantly to the development of cytokine release syndrome [60]. Compared to previous studies with 4-1BB-CD3 ζ [61], CD28-OX40-CD3 ζ [62], and TRUCK CD28-4-1BB-CD3 ζ [63] GD2.CAR T cells, our CD28-CD3 ζ -GITRL GD2.CAR T cells demonstrate a safer and more moderate cytokine profile. In addition, our CAR T cells can secrete a greater amount of granzymes relative to other effector molecules and cytokines. Moreover, our *in vivo* experiments revealed a safety profile with no observed toxicity.

A pattern of granzyme A, granzyme B, and perforin secretion was observed, consistent with the functional differentiation of memory T cells. Effector molecules secreted by the GD2.CAR T cells were in the order of GrmA < GrmB < Per, indicating cell differentiation towards effector or effector memory [64]. In addition, transcriptional analysis revealed a signature of memory phenotype change. We also observed downregulation of *GZMA*, *GZMK*, and *PRF1* gene expression without a signature of cell exhaustion. Furthermore, cytokine analysis demonstrated the ability of GD2.CAR T cells to efficiently produce proteins. Thus, the results indicate an early phenotypic shift of GD2.CAR T cells towards Tem cells during their initial interaction with tumors, with no evidence of functional aberration. On the other hand, stimulation of GD2.CAR T cells with anti-CD3/CD28 and IL-2 could promote the accumulation of effector molecules in granules [65], which may explain the observed upregulation of effector molecules before interaction with tumors. Expression of the *IFNG* gene was also upregulated. Memory effector T cells exhibit a greater capacity for IFN- γ release compared to central memory T cells [66], suggesting the possible acquisition of a cytotoxic effector phenotype by CAR T cells after co-culture with tumors. Additionally, prior research has demonstrated that induction of GITR ligand expression on CAR T cells results in enhanced production of IFN- γ .

Several features of the transcriptome of GD2.CAR T cells were identified following their initial interaction with GD2-positive tumor cell lines. Specifically, chemokine signatures were detected in CAR T cells, suggesting a T cell chemokine response to an antigen [67]. We propose that one of the key steps in early CAR T cell-tumor interaction is the recruitment of other effector cells to the site of the lesion. A recent study showed that expression of chemokine and cytokine receptor genes is upregulated following anti-CD3/CD28 and IL-2 stimulation [68]. However, we found these genes were downregulated in CAR T cells after co-culture with tumor. Therefore, the incorporation of chemokine receptors into CAR T cell constructs may be a promising approach for further research [69]. GSEA analysis revealed the involvement of cytokine-mediated signaling pathways, cellular response to IFN- γ , and IFN- γ -mediated signaling pathways during early stages of the GD2.CAR T cell interaction with melanoma, possibly contributing to antitumor immunity. We also observed that GD2.CAR T cells could efficiently kill tumor cells *in vitro* and effectively control tumor growth *in vivo*, thus confirming the cytotoxic potential of transduced cells.

In summary, our findings provide robust preclinical evidence for the potential of GD2-specific CAR T cells as a therapeutic strategy for melanoma. Although it has provided valuable insights, our *in vivo* study was limited to a xenograft model utilizing a single tumor cell line (SK-MEL-37). Therefore, it is important to acknowledge this model cannot fully replicate the complexity of the human TME, nor the heterogeneity of human melanoma. Success-

ful clinical translation will require further investigations to overcome these limitations. Future research should prioritize strategies for increasing the migration of CAR T cells to the tumor site, improving their resistance to inhibitory signals within the TME, and promoting the development of a long-lived memory phenotype. Additional studies employing a broader range of melanoma models, including patient-derived xenografts and those evaluating systemic delivery, will be crucial for assessing long-term efficacy and safety, thus paving the way for clinical trials.

5. Conclusion

GD2-specific CAR T cells generated and characterized using advanced techniques showed potent *in vitro* and *in vivo* antitumor activity against melanoma. The phenotypic and functional characteristics of these cells, including a naive-to-effector transition and strong cytotoxic potential, highlight their potential as an effective therapeutic strategy warranting further clinical development.

Availability of Data and Materials

The datasets generated and analyzed during the current study are accessible from the corresponding author upon email request.

Author Contributions

HS conceptualized and initiated the study, and provided materials (retroviral vector, tumor cell lines). SS, JS, and JP designed the research study and reviewed the literature. VK managed donor recruitment. JP, JS, MF, SA, AA, JL, MV, EZ, and OS performed the investigation and formal analysis: JP, JS, and MF conducted CAR T cell production and tumor cell line culture; JP, JS, and JL performed *in vitro* co-culture experiments (flow cytometry, LDH and cytokine analysis, magnetic sorting); SA, AA, and MV conducted NanoString gene expression analysis; EZ and OS performed *in vivo* experiments. RPZ, SA, JP, and JS analyzed and visualized the data. SA, RPZ, OPZ, and MV conducted differential gene expression, HSNE, and GSEA analyses. RPZ, SA, JP, and AA prepared the figures. JP wrote the original draft. JP, SS, JS, AA, SA, RPZ, and VK revised and edited the manuscript. All authors contributed to editorial changes in the manuscript. All authors read and approved the final manuscript. All authors have participated sufficiently in the work and agreed to be accountable for all aspects of the work.

Ethics Approval and Consent to Participate

The study was carried out in accordance with the guidelines of the Declaration of Helsinki and was approved by the local ethics committee of the Research Institute of Fundamental and Clinical Immunology at a meeting on May 30, 2022 [protocol #139]. This approval encompassed all procedures involving human participants and laboratory animals, including the collection of blood samples from

healthy adult donors, the use of human biomaterials (including human-derived cell lines S6 and V9), and the conduct of animal experiments. All animal experiments were conducted in accordance with the European Community Directive (86/609/EEC) and the standards of humane treatment. All healthy blood donors provided written informed consent for their participation in this study, including the use of their samples in research.

Acknowledgment

Not applicable.

Funding

This study was supported by Research Work [project #124112200103-3] “The investigation of the role of molecular-cellular interactions in immunoregulation and the substantiation of new immunotherapy technologies”.

Conflict of Interest

The authors declare no conflict of interest.

Supplementary Material

Supplementary material associated with this article can be found, in the online version, at <https://doi.org/10.31083/FBL41221>.

References

- [1] Erdei E, Torres SM. A new understanding in the epidemiology of melanoma. *Expert Review of Anticancer Therapy*. 2010; 10: 1811–1823. <https://doi.org/10.1586/era.10.170>.
- [2] Baloghová J, Michalková R, Baranová Z, Mojžišová G, Fedáková Z, Mojžiš J. Spice-Derived Phenolic Compounds: Potential for Skin Cancer Prevention and Therapy. *Molecules* (Basel, Switzerland). 2023; 28: 6251. <https://doi.org/10.3390/molecules28176251>.
- [3] Prendergast CM, Capaccione KM, Lopci E, Das JP, Shoushtari AN, Yeh R, *et al.* More than Just Skin-Deep: A Review of Imaging’s Role in Guiding CAR T-Cell Therapy for Advanced Melanoma. *Diagnostics* (Basel, Switzerland). 2023; 13: 992. <https://doi.org/10.3390/diagnostics13050992>.
- [4] Bernatchez C, Radvanyi LG, Hwu P. Advances in the treatment of metastatic melanoma: adoptive T-cell therapy. *Seminars in Oncology*. 2012; 39: 215–226. <https://doi.org/10.1053/j.seminocol.2012.01.006>.
- [5] Verma A, Rafiq S. Chimeric Antigen Receptor (CAR) T Cell Therapy for Glioblastoma. *Cancer Treatment and Research*. 2022; 183: 161–184. https://doi.org/10.1007/978-3-030-96376-7_5.
- [6] Zhou S, Sun H, Choi SI, Yin J. Present Status and Advances in Chimeric Antigen Receptor T Cell Therapy for Glioblastoma. *Frontiers in Bioscience* (Landmark Edition). 2023; 28: 206. <https://doi.org/10.31083/j.fbl2809206>.
- [7] Hersey P, Jamal O, Henderson C, Zardawi I, D’Alessandro G. Expression of the gangliosides GM3, GD3 and GD2 in tissue sections of normal skin, naevi, primary and metastatic melanoma. *International Journal of Cancer*. 1988; 41: 336–343. <https://doi.org/10.1002/ijc.2910410303>.
- [8] Philippova J, Shevchenko J, Sennikov S. GD2-targeting therapy: a comparative analysis of approaches and promising directions. *Frontiers in Immunology*. 2024; 15: 1371345. <https://doi.org/10.3389/fimmu.2024.1371345>.
- [9] Ohmi Y, Kambe M, Ohkawa Y, Hamamura K, Tajima O, Takeuchi R, *et al.* Differential roles of gangliosides in malignant properties of melanomas. *PLoS One*. 2018; 13: e0206881. <https://doi.org/10.1371/journal.pone.0206881>.
- [10] Yesmin F, Bhuiyan RH, Ohmi Y, Yamamoto S, Kaneko K, Ohkawa Y, *et al.* Ganglioside GD2 Enhances the Malignant Phenotypes of Melanoma Cells by Cooperating with Integrins. *International Journal of Molecular Sciences*. 2021; 23: 423. <https://doi.org/10.3390/ijms23010423>.
- [11] Strobel SB, Machiraju D, Hülsmeier I, Becker JC, Paschen A, Jäger D, *et al.* Expression of Potential Targets for Cell-Based Therapies on Melanoma Cells. *Life* (Basel, Switzerland). 2021; 11: 269. <https://doi.org/10.3390/life11040269>.
- [12] Yvon E, Del Vecchio M, Savoldo B, Hoyos V, Dutour A, Anichini A, *et al.* Immunotherapy of metastatic melanoma using genetically engineered GD2-specific T cells. *Clinical Cancer Research: an Official Journal of the American Association for Cancer Research*. 2009; 15: 5852–5860. <https://doi.org/10.1158/1078-0432.CCR-08-3163>.
- [13] Yu J, Wu X, Yan J, Yu H, Xu L, Chi Z, *et al.* Anti-GD2/4-1BB chimeric antigen receptor T cell therapy for the treatment of Chinese melanoma patients. *Journal of Hematology & Oncology*. 2018; 11: 1. <https://doi.org/10.1186/s13045-017-0548-2>.
- [14] Gargett T, Yu W, Dotti G, Yvon ES, Christo SN, Hayball JD, *et al.* GD2-specific CAR T Cells Undergo Potent Activation and Deletion Following Antigen Encounter but can be Protected From Activation-induced Cell Death by PD-1 Blockade. *Molecular Therapy: the Journal of the American Society of Gene Therapy*. 2016; 24: 1135–1149. <https://doi.org/10.1038/mt.2016.63>.
- [15] Philippova JG, Kuznetsova MS, Shevchenko YuA, Tereshchenko VP, Fisher MS, Kurilin VV, *et al.* Phenotype and effector functions of GD2-specific CAR-T lymphocytes in vitro. *Immunologiya*. 2022; 43: 525–535. <https://doi.org/10.33029/0206-4952-2022-43-5-525-535>. (In Russian)
- [16] Brown M, Gargett T. CARPETS: A Phase I study of the safety and immune effects of an escalating dose of autologous GD2 chimeric antigen receptor-expressing peripheral blood T cells in patients with GD2-positive metastatic melanoma and refractory solid tumors [abstract]. *Cancer Research*. 2019; 79: Abstract nr CT118. <https://doi.org/10.1158/1538-7445.AM2019-CT118>.
- [17] Alsalloum A, Alrhoun S, Shevchenko J, Fisher M, Philippova J, Perik-Zavodskii R, *et al.* TCR-Engineered Lymphocytes Targeting NY-ESO-1: In Vitro Assessment of Cytotoxicity against Tumors. *Biomedicines*. 2023; 11: 2805. <https://doi.org/10.3390/biomedicines11102805>.
- [18] Alsalloum A, Shevchenko J, Fisher M, Philippova J, Perik-Zavodskii R, Perik-Zavodskaja O, *et al.* Exploring TCR-like CAR-Engineered Lymphocyte Cytotoxicity against MAGE-A4. *International Journal of Molecular Sciences*. 2023; 24: 15134. <https://doi.org/10.3390/ijms242015134>.
- [19] Wang Y, Wang L, Seo N, Okumura S, Hayashi T, Akahori Y, *et al.* CAR-Modified Vγ9Vδ2 T Cells Propagated Using a Novel Bisphosphonate Prodrug for Allogeneic Adoptive Immunotherapy. *International Journal of Molecular Sciences*. 2023; 24: 10873. <https://doi.org/10.3390/ijms241310873>.
- [20] Tian J, Zhang B, Rui K, Wang S. The Role of GITR/GITRL Interaction in Autoimmune Diseases. *Frontiers in Immunology*. 2020; 11: 588682. <https://doi.org/10.3389/fimmu.2020.588682>.
- [21] Melsen JE, van Ostaïen-Ten Dam MM, Lankester AC, Schilham MW, van den Akker EB. A Comprehensive Workflow for Applying Single-Cell Clustering and Pseudotime Analysis to Flow Cytometry Data. *Journal of Immunology* (Baltimore, Md.: 1950). 2020; 205: 864–871. <https://doi.org/10.4049/jimmunol.1901530>.
- [22] Höllt T, Pezzotti N, van Unen V, Koning F, Eisemann E, Lelieveldt B, *et al.* Cytosplore: Interactive Immune Cell Pheno-

- typing for Large Single-Cell Datasets. *Computer Graphics Forum*. 2016; 35: 171–180. <https://doi.org/10.1111/cgf.12893>.
- [23] Fang Z, Liu X, Peltz G. GSEAPy: a comprehensive package for performing gene set enrichment analysis in Python. *Bioinformatics* (Oxford, England). 2023; 39: btac757. <https://doi.org/10.1093/bioinformatics/btac757>.
- [24] Mangare C, Tischer-Zimmermann S, Riese SB, Dragon AC, Prinz I, Blasczyk R, *et al.* Robust Identification of Suitable T-Cell Subsets for Personalized CMV-Specific T-Cell Immunotherapy Using CD45RA and CD62L Microbeads. *International Journal of Molecular Sciences*. 2019; 20: 1415. <https://doi.org/10.3390/ijms20061415>.
- [25] Harari-Steinfeld R, Abhinav Ayyadevara VSS, Cuevas L, Marincola F, Roh KH. Standardized *in-vitro* evaluation of CAR-T cells using acellular artificial target particles. *Frontiers in Immunology*. 2022; 13: 994532. <https://doi.org/10.3389/fimmu.2022.994532>.
- [26] Cibrián D, Sánchez-Madrid F. CD69: from activation marker to metabolic gatekeeper. *European Journal of Immunology*. 2017; 47: 946–953. <https://doi.org/10.1002/eji.201646837>.
- [27] Liu X, Zhu Z, Wang X. Specificity and function of T cell subset identities using single-cell sequencing. *Clinical and Translational Discovery*. 2023; 3: e199. <https://doi.org/10.1002/ctd2.199>.
- [28] Lagumdzic E, Pernold C, Viano M, Olgiati S, Schmitt MW, Mair KH, *et al.* Transcriptome Profiling of Porcine Naïve, Intermediate and Terminally Differentiated CD8⁺ T Cells. *Frontiers in Immunology*. 2022; 13: 849922. <https://doi.org/10.3389/fimmu.2022.849922>.
- [29] Tay NQ, Lee DCP, Chua YL, Prabhu N, Gascoigne NRJ, Kemeny DM. CD40L Expression Allows CD8⁺ T Cells to Promote Their Own Expansion and Differentiation through Dendritic Cells. *Frontiers in Immunology*. 2017; 8: 1484. <https://doi.org/10.3389/fimmu.2017.01484>.
- [30] Ward-Kavanagh LK, Lin WW, Šedý JR, Ware CF. The TNF Receptor Superfamily in Co-stimulating and Co-inhibitory Responses. *Immunity*. 2016; 44: 1005–1019. <https://doi.org/10.1016/j.immuni.2016.04.019>.
- [31] Gattinoni L, Ji Y, Restifo NP. Wnt/beta-catenin signaling in T-cell immunity and cancer immunotherapy. *Clinical Cancer Research: an Official Journal of the American Association for Cancer Research*. 2010; 16: 4695–4701. <https://doi.org/10.1158/1078-0432.CCR-10-0356>.
- [32] Gattinoni L, Zhong XS, Palmer DC, Ji Y, Hinrichs CS, Yu Z, *et al.* Wnt signaling arrests effector T cell differentiation and generates CD8⁺ memory stem cells. *Nature Medicine*. 2009; 15: 808–813. <https://doi.org/10.1038/nm.1982>.
- [33] Yoshida K, Sakamoto A, Yamashita K, Arguni E, Horigome S, Arima M, *et al.* Bcl6 controls granzyme B expression in effector CD8⁺ T cells. *European Journal of Immunology*. 2006; 36: 3146–3156. <https://doi.org/10.1002/eji.200636165>.
- [34] Maasho K, Masilamani M, Valas R, Basu S, Coligan JE, Borrego F. The inhibitory leukocyte-associated Ig-like receptor-1 (LAIR-1) is expressed at high levels by human naive T cells and inhibits TCR mediated activation. *Molecular Immunology*. 2005; 42: 1521–1530. <https://doi.org/10.1016/j.molimm.2005.01.004>.
- [35] Abadier M, Ley K. P-selectin glycoprotein ligand-1 in T cells. *Current Opinion in Hematology*. 2017; 24: 265–273. <https://doi.org/10.1097/MOH.0000000000000331>.
- [36] Zhang Y, Guan XY, Jiang P. Cytokine and Chemokine Signals of T-Cell Exclusion in Tumors. *Frontiers in Immunology*. 2020; 11: 594609. <https://doi.org/10.3389/fimmu.2020.594609>.
- [37] McPherson AJ, Snell LM, Mak TW, Watts TH. Opposing roles for TRAF1 in the alternative versus classical NF-κB pathway in T cells. *The Journal of Biological Chemistry*. 2012; 287: 23010–23019. <https://doi.org/10.1074/jbc.M112.350538>.
- [38] Snell LM, McPherson AJ, Lin GHY, Sakaguchi S, Pandolfi PP, Riccardi C, *et al.* CD8 T cell-intrinsic GITR is required for T cell clonal expansion and mouse survival following severe influenza infection. *Journal of Immunology* (Baltimore, Md.: 1950). 2010; 185: 7223–7234. <https://doi.org/10.4049/jimmunol.1001912>.
- [39] Wagle MV, Vervoort SJ, Kelly MJ, Van Der Byl W, Peters TJ, Martin BP, *et al.* Antigen-driven EGR2 expression is required for exhausted CD8⁺ T cell stability and maintenance. *Nature Communications*. 2021; 12: 2782. <https://doi.org/10.1038/s41467-021-23044-9>.
- [40] Symonds ALJ, Miao T, Busharat Z, Li S, Wang P. Egr2 and 3 maintain anti-tumour responses of exhausted tumour infiltrating CD8⁺ T cells. *Cancer Immunology, Immunotherapy: CII*. 2023; 72: 1139–1151. <https://doi.org/10.1007/s00262-022-03319-w>.
- [41] Ashouri JF, Lo WL, Nguyen TTT, Shen L, Weiss A. ZAP70, too little, too much can lead to autoimmunity. *Immunological Reviews*. 2022; 307: 145–160. <https://doi.org/10.1111/imr.13058>.
- [42] Palmer DC, Guittard GC, Franco Z, Crompton JG, Eil RL, Patel SJ, *et al.* Cish actively silences TCR signaling in CD8⁺ T cells to maintain tumor tolerance. *The Journal of Experimental Medicine*. 2015; 212: 2095–2113. <https://doi.org/10.1084/jem.20150304>.
- [43] Lv J, Qin L, Zhao R, Wu D, Wu Z, Zheng D, *et al.* Disruption of CISH promotes the antitumor activity of human T cells and decreases PD-1 expression levels. *Molecular Therapy Oncolytics*. 2022; 28: 46–58. <https://doi.org/10.1016/j.omto.2022.12.003>.
- [44] O'Connell P, Hyslop S, Blake MK, Godbehere S, Amalfitano A, Aldhamen YA. SLAMF7 Signaling Reprograms T Cells toward Exhaustion in the Tumor Microenvironment. *Journal of Immunology* (Baltimore, Md.: 1950). 2021; 206: 193–205. <https://doi.org/10.4049/jimmunol.2000300>.
- [45] Orning P, Lien E. Multiple roles of caspase-8 in cell death, inflammation, and innate immunity. *Journal of Leukocyte Biology*. 2021; 109: 121–141. <https://doi.org/10.1002/JLB.3MR0420-305R>.
- [46] Lee YG, Guruprasad P, Ghilardi G, Pajarillo R, Sauter CT, Patel R, *et al.* Modulation of BCL-2 in Both T Cells and Tumor Cells to Enhance Chimeric Antigen Receptor T-cell Immunotherapy against Cancer. *Cancer Discovery*. 2022; 12: 2372–2391. <https://doi.org/10.1158/2159-8290.CD-21-1026>.
- [47] Yin X, He L, Guo Z. T-cell exhaustion in CAR-T-cell therapy and strategies to overcome it. *Immunology*. 2023; 169: 400–411. <https://doi.org/10.1111/imm.13642>.
- [48] Gattinoni L, Lugli E, Ji Y, Pos Z, Paulos CM, Quigley MF, *et al.* A human memory T cell subset with stem cell-like properties. *Nature Medicine*. 2011; 17: 1290–1297. <https://doi.org/10.1038/nm.2446>.
- [49] Tay RE, Richardson EK, Toh HC. Revisiting the role of CD4⁺ T cells in cancer immunotherapy-new insights into old paradigms. *Cancer Gene Therapy*. 2021; 28: 5–17. <https://doi.org/10.1038/s41417-020-0183-x>.
- [50] Alizadeh D, Wang D, Brown CE. Uncovering the Role of CD4⁺ CAR T Cells in Cancer Immunotherapy. *Cancer Research*. 2023; 83: 2813–2815. <https://doi.org/10.1158/0008-5472.CA.N-23-1948>.
- [51] Benmebarek MR, Karches CH, Cadilha BL, Lesch S, Endres S, Kobold S. Killing Mechanisms of Chimeric Antigen Receptor (CAR) T Cells. *International Journal of Molecular Sciences*. 2019; 20: 1283. <https://doi.org/10.3390/ijms20061283>.
- [52] Cheng M., Bergsbaken T. Investigating tissue-resident memory T cell differentiation of CAR T cells reveals an unexpected role for CD69 [abstract]. *Cancer Research*. 2023; 83: Abstract nr 896. <https://doi.org/10.1158/1538-7445.AM2023-896>.
- [53] Ugolini A, Nuti M. CD137⁺ T-Cells: Protagonists of the Immunotherapy Revolution. *Cancers*. 2021; 13: 456. <https://doi.org/10.3390/cancers13030456>.
- [54] Barao I. The TNF receptor-ligands 4-1BB-4-1BBL and GITR-GITRL in NK cell responses. *Frontiers in Immunology*. 2013; 3:

402. <https://doi.org/10.3389/fimmu.2012.00402>.
- [55] Ephrem A, Epstein AL, Stephens GL, Thornton AM, Glass D, Shevach EM. Modulation of Treg cells/T effector function by GITR signaling is context-dependent. *European Journal of Immunology*. 2013; 43: 2421–2429. <https://doi.org/10.1002/eji.201343451>.
- [56] Konkel JE, Zhang D, Zanvit P, Chia C, Zangarile-Murray T, Jin W, *et al.* Transforming Growth Factor- β Signaling in Regulatory T Cells Controls T Helper-17 Cells and Tissue-Specific Immune Responses. *Immunity*. 2017; 46: 660–674. <https://doi.org/10.1016/j.immuni.2017.03.015>.
- [57] Tang M, Jia F, Nan F, Zuo F, Yuan Z, Zhang D. Role of Cytokines in Thymic Regulatory T Cell Generation: Overview and Updates. *Frontiers in Immunology*. 2022; 13: 883560. <https://doi.org/10.3389/fimmu.2022.883560>.
- [58] Damen H, Tebid C, Viens M, Roy DC, Dave VP. Negative Regulation of Zap70 by Lck Forms the Mechanistic Basis of Differential Expression in CD4 and CD8 T Cells. *Frontiers in Immunology*. 2022; 13: 935367. <https://doi.org/10.3389/fimmu.2022.935367>.
- [59] Lo WL, Weiss A. Adapting T Cell Receptor Ligand Discrimination Capability *via* LAT. *Frontiers in Immunology*. 2021; 12: 673196. <https://doi.org/10.3389/fimmu.2021.673196>.
- [60] Wei Z, Cheng Q, Xu N, Zhao C, Xu J, Kang L, *et al.* Investigation of CRS-associated cytokines in CAR-T therapy with meta-GNN and pathway crosstalk. *BMC Bioinformatics*. 2022; 23: 373. <https://doi.org/10.1186/s12859-022-04917-2>.
- [61] Prapa M, Chiavelli C, Golinelli G, Grisendi G, Bestagno M, Di Tinco R, *et al.* GD2 CAR T cells against human glioblastoma. *NPJ Precision Oncology*. 2021; 5: 93. <https://doi.org/10.1038/s41698-021-00233-9>.
- [62] Gargett T, Ebert LM, Truong NTH, Kollis PM, Sedivakova K, Yu W, *et al.* GD2-targeting CAR-T cells enhanced by transgenic IL-15 expression are an effective and clinically feasible therapy for glioblastoma. *Journal for Immunotherapy of Cancer*. 2022; 10: e005187. <https://doi.org/10.1136/jitc-2022-005187>.
- [63] Glienke W, Dragon AC, Zimmermann K, Martyniszyn-Eiben A, Mertens M, Abken H, *et al.* GMP-Compliant Manufacturing of TRUCKs: CAR T Cells targeting GD₂ and Releasing Inducible IL-18. *Frontiers in Immunology*. 2022; 13: 839783. <https://doi.org/10.3389/fimmu.2022.839783>.
- [64] Takata H, Takiguchi M. Three memory subsets of human CD8+ T cells differently expressing three cytolytic effector molecules. *Journal of Immunology (Baltimore, Md.: 1950)*. 2006; 177: 4330–4340. <https://doi.org/10.4049/jimmunol.177.7.4330>.
- [65] Hay ZLZ, Slansky JE. Granzymes: The Molecular Executors of Immune-Mediated Cytotoxicity. *International Journal of Molecular Sciences*. 2022; 23: 1833. <https://doi.org/10.3390/ijms23031833>.
- [66] Märkl F, Benmeharek MR, Keyl J, Cadilha BL, Geiger M, Karches C, *et al.* Bispecific antibodies redirect synthetic agonistic receptor modified T cells against melanoma. *Journal for Immunotherapy of Cancer*. 2023; 11: e006436. <https://doi.org/10.1136/jitc-2022-006436>.
- [67] Eberlein J, Davenport B, Nguyen TT, Victorino F, Jhun K, van der Heide V, *et al.* Chemokine Signatures of Pathogen-Specific T Cells I: Effector T Cells. *Journal of Immunology (Baltimore, Md.: 1950)*. 2020; 205: 2169–2187. <https://doi.org/10.4049/jimmunol.2000253>.
- [68] Lee JH, Lee BH, Jeong S, Joh CSY, Nam HJ, Choi HS, *et al.* Single-cell RNA sequencing identifies distinct transcriptomic signatures between PMA/ionomycin- and α CD3/ α CD28-activated primary human T cells. *Genomics & Informatics*. 2023; 21: e18. <https://doi.org/10.5808/gi.23009>.
- [69] Wang Y, Wang J, Yang X, Yang J, Lu P, Zhao L, *et al.* Chemokine Receptor CCR2b Enhanced Anti-tumor Function of Chimeric Antigen Receptor T Cells Targeting Mesothelin in a Non-small-cell Lung Carcinoma Model. *Frontiers in Immunology*. 2021; 12: 628906. <https://doi.org/10.3389/fimmu.2021.628906>.